

See discussions, stats, and author profiles for this publication at: <https://www.researchgate.net/publication/319509271>

# Time-Frequency-Based Analysis of Pedestrian Induced Vibrations Using a Two-Step Clustering Approach

Conference Paper · September 2017

DOI: 10.24904/footbridge2017.09354

---

CITATIONS

0

---

READS

49

3 authors, including:



**Arndt Goldack**

Technische Universität Berlin

17 PUBLICATIONS 35 CITATIONS

SEE PROFILE



**Sriram Narasimhan**

University of Waterloo

81 PUBLICATIONS 1,305 CITATIONS

SEE PROFILE

10.24904/footbridge2017.09354

## TIME-FREQUENCY-BASED ANALYSIS OF PEDESTRIAN INDUCED VIBRATION USING A TWO-STEP CLUSTERING APPROACH

**Arndt GOLDACK**

Researcher  
TU Berlin  
Berlin, Germany

[arndt.goldack@tu-berlin.de](mailto:arndt.goldack@tu-berlin.de)

**Andreas JANSEN**

Structural Engineer  
GMG Ingenieurgesellschaft  
Berlin, Germany

[andreas.jansen@gmg-berlin.de](mailto:andreas.jansen@gmg-berlin.de)

**Sriram NARASIMHAN**

Associate Professor  
University of Waterloo  
Waterloo, Canada

[snarasim@uwaterloo.ca](mailto:snarasim@uwaterloo.ca)

### Summary

Vibration of footbridges caused by walking pedestrians is still an important research topic. The excitation is very complex and recent load models have been shown to be sometimes un-conservative. Furthermore, cable-supported footbridges and stress ribbon footbridges have closely spaced natural frequencies. Well-known methods for modal identification such frequency domain decomposition, subspace identification and blind source separation require comparatively long time series to work well under such conditions. They sometimes have problems with transient frequency components of pedestrian induced vibrations. This paper presents a novel method to analyze the vibration of highly flexible footbridges. This method addresses three aspects: analyzing measurement data to understand the mechanics of the excitation, comparing the quality of load models with recorded measurements in the time-frequency domain and identifying modal parameters such as natural frequencies and mode shapes. This method utilizes time-frequency analysis and a two-step clustering approach for analysis. The implementation and advantages of this method are discussed using vibration data from an aluminum bridge at the University of Waterloo and a stress ribbon bridge at the TU Berlin. Furthermore, some interesting findings for pedestrian induced vibrations of both bridges are presented.

**Keywords:** human-induced vibrations; footbridge dynamics; time-frequency analysis; clustering; DBSCAN; operational modal identification; load model

### 1. Introduction

This paper presents a novel method to analyze the vibration response of highly flexible footbridges due to walking pedestrians. This method addresses three main aspects: analyzing measurement data to understand the mechanics of the excitation, comparing the quality of load models with recorded measurements in the time-frequency domain and identifying modal properties of structures such as natural frequencies and mode shapes.

Lightweight footbridges such as aluminum bridges, cable stayed bridges and stress ribbon bridges are prone to pedestrian induced vibrations due to their low mass and high flexibility. Their vibration response contains a mixture of transient and stationary oscillatory components. Furthermore, some of these footbridges have closely spaced natural frequencies. Several studies by the authors showed that this complex excitation in combination with closely spaced modes is very difficult to obtain good modal identification results.

For structural engineers it is important to have reliable load models to calculate the vibration response already during the conceptual design of footbridges. However, it was reported that in some cases the load models recommend by Hivoss [1] are un-conservative when compared with actual measurements [2]. Consequently, load models for pedestrian induced vibration are still under investigation. Often, the contact forces of walking persons are measured on treadmills and analyzed using Fourier series. Recently, the

responses of vibrating footbridges have been used to estimate the parameters for the load models. The proposed method can be utilized to evaluate these load models and their parameters.

The proposed method is based on the assumption that a combination of free and forced vibrations describes the majority of vibration problems in structural dynamics using the framework of modal analysis. This is also valid for pedestrian induced vibrations of footbridges. In this paper the response vector  $x(t)$  of a vibrating footbridge is assumed to be a linear combination of mixing vectors  $a_q$  also called shape functions and the sources  $s_q(t)$ . When the response signal is the only available information, the estimation of the mixing vectors and sources is referred to as blind source separation (BSS) [3]. Generally stated, the problem of BSS is to estimate  $Q$  mixed sources  $s(t) = [s_1(t), s_2(t), \dots, s_Q(t)]^T$  from  $P$  observation  $x(t) = [x_1(t), x_2(t), \dots, x_P(t)]^T$ . The sources are mixed according to a  $P \times Q$  mixing matrix  $A$ , such that:

$$x(t) = A \cdot s(t) = \sum_{q=1}^Q a_q \cdot s_q(t) \quad (1)$$

The response vector  $x(t)$  can be a time series of acceleration, velocity or displacement depending on the measurements. In this paper acceleration measurements were used. It shall be noted, that a source  $s_q(t)$  can be a combination of a natural frequency and different excitation frequencies from forced vibration. In the context of modal identification, the vectors  $a_q$  are often referred to as mode shapes [3]. In this paper, the general term mixing vectors is chosen because they are not calculated by solving an eigenvalue problem or using a Singular Value Decomposition (SVD).

In the following sections the proposed method is fully described and discussed. In section 2 the novel method is explained stepwise. The method is applied to a 22.9 m span Aluminum bridge and a 13 m CFRP-stress ribbon bridge in section 3. The main conclusions of this paper are drawn in section 4.

## 2. Methodology

Well-known and widely used methods to analyze time series such as the Fourier Analysis or methods for modal identification, including frequency domain decomposition and stochastic subspace identification, require comparatively long and stationary time-series to reliably identify the characteristic frequencies and the associated modes. Transient components and changes in frequency as well as in mode shapes are difficult to detect, because the results are averaged over a long or the entire duration of the measurement.

With time-frequency analysis, it is possible to identify and visualize non-stationary frequency content in three-dimensional time-frequency maps, because small time windows of the entire measurements are analyzed. In recent years, time-frequency analysis has been applied to vibration problems in structural engineering [4], [5], [6], [7], [8]. Le and Paultre [7] introduced the Time-Frequency Domain Decomposition (TFDD), which involves the application of the *Continuous Wavelet Transform* (CWT) to the correlation matrix of signals from ambient excitation and a SVD to obtain singular values and singular vectors. Frequency components in the signal are identified as ridges in the first singular value of the wavelet coefficients. The accompanying singular vector gives the mode shape estimate at every point in the time-frequency plane. While the TFDD performs well in modal identification from the response of ambient excitation, the authors faced difficulties when applying it to pedestrian induced vibration of lightweight footbridges.

The proposed method involves the application of a time frequency transform such as the CWT directly to the signal and a subsequent ridge detection algorithm. Instead of applying a SVD, the mixing vectors are estimated for all ridge points using the time frequency coefficients of the time frequency transform for each sensor. Then, a two-step clustering with the DBSCAN algorithm is applied. The clustering uses the shape of the mixing vector and the frequency components of the sources as similarity measures. This enables the detection of different mixing vectors, which may occur at nearly the same frequency. This proved to be very relevant in the context of cable-supported footbridges with closely space natural frequencies.

In the following section, the five steps of the proposed method are outlined and discussed.

## 2.1 Step 1: Time Frequency Representation (TFR) and the Average Power Spectrum (APS)

There are various methods to obtain the Time-Frequency Representation (TFR) of a signal such as the short time Fourier Transformation (STFT) [9], the continuous wavelet transform (CWT) [10] or the S-Transform (ST) by Stockwell et al. [11]. The choice of a particular time-frequency transform depends on several factors such as the bandwidth and characteristics of a signal, desired time-frequency resolution and computational efficiency [12]. All TF transformations suffer from computational artifacts, e.g. end-effects or cross-terms. These effects can distort the time-frequency representation of oscillatory components in a signal or result in the appearance of components that do not have a physical meaning. It has been found that computational artifacts appear over time intervals where the signal is non-stationary, e.g. if a component starts or ends. Moreover, due to the discontinuity of an oscillatory component, closely spaced frequencies can be affected. It is important to have these artificial effects in mind when analyzing a TFR.

This study uses the well-established CWT, which shall be introduced briefly. For further information the interested reader is referred to [13, 14, 15]. The wavelet transform  $W(t,a)$  of the signal  $x(t)$  is defined as:

$$W(t,a) = \int_{-\infty}^{\infty} x(\tau) \frac{1}{\sqrt{a}} \psi^* \left( \frac{\tau-t}{a} \right) d\tau \quad (2)$$

with the complex conjugate  $\psi^*(t/a)$  of the mother wavelet  $\psi(t/a)$  and the scale parameter  $a$ . The wavelet spectrum of a signal is obtained by calculating the wavelet transform  $W(t,a)$  over a set of scale parameters  $a$ . In this study, the mother wavelet is the complex Morlet wavelet in Eq. 3. Herein, the center frequency  $\omega_0$  determines where the mother-wavelet is centered. For example, a center frequency of  $\omega_0 = 44 \text{ rad/s}$  ( $f_0 = 7 \text{ Hz}$ ) proves suitable for the bandwidth between 0 Hz and 15 Hz. In order to get a time-frequency rather than a time-scale parameter representation, it is necessary to translate the scale parameter into frequencies with Eq. 4 for the complex Morlet wavelet.

$$\psi \left( \frac{t}{a} \right) = \pi^{-\frac{1}{4}} e^{-i\omega_0 \frac{t}{a}} e^{-\frac{t^2}{2a^2}} \quad (3)$$

$$f(a) = \frac{f_0 + \sqrt{\frac{1}{2}\pi^{-2} + f_0^2}}{2a} \quad (4)$$

The squared absolute wavelet coefficients  $|W(t,f)|^2$  - a measure for power - of each acceleration sensor are plotted over the time and frequency axes in Power Spectrum (PS) diagrams. Regions with high oscillation energy can be easily identified in the power spectrum.

For further processing, the Average Power Spectrum (APS) is calculated according to Eq. 5 adding the PS of all  $P$  individual sensors. In doing so, the TFR of all sensors are mapped into one diagram.

$$APS(t, f) = \frac{1}{P} \sum_{p=1}^P |W_p(t, f)|^2 \quad (5)$$

In contrast to Fourier Analysis the wavelet amplitude is not directly connected the amplitude of harmonic components in the signal. Therefore, the resulting TFR allows only a qualitative evaluation. Consequently, the APS will be presented without units and normalized to unity.

## 2.2 Step 2: Ridge Detection – search for local maxima

A chain of peaks of high-energy regions in the PS or APS is referred to as ridge. Identifying ridges allows for a clearer picture of the signal's frequency content over time. The points of ridges are detected in the APS with a simple ridge detection method [12, 16] that determines local maxima. A slice in the APS at a certain time is a curve in the  $f$ - $W^2$  plane, which is derived two times to find local maxima. In doing so, a set of

maxima (peaks) as well as their coordinates in the time-frequency plane  $(t_R, f_R)$  are determined. In addition, the maxima must be greater than a certain threshold value to eliminate noise.

### 2.3 Step 3: Calculation of mixing vectors

Once the ridges are identified in the APS, the current state of the complex mixing vectors can be estimated for all ridge points. The mixing vector  $a_e(t_r, f_r)$  at a certain ridge point  $(t_R, f_R)$  calculates according Eq. 6. The ratio between the time-frequency coefficients  $c_p = W_1(t_R, f_R)$  for  $p > 1$  of the TFR of the sensor  $p$  and the reference time-frequency coefficients  $c_1 = W_1(t_R, f_R)$  of the TFR of the reference sensor [4, 6]. The real valued mixing vectors are obtained in accordance to Eq. 6 and Eq. 7 by considering the absolute value of the time-frequency coefficients  $c_p$  and the phase difference with the reference observation [13, 14].

$$a_e(t_R, f_R) = \begin{bmatrix} 1.0 \\ c_2 / c_1 \\ \vdots \\ c_p / c_1 \end{bmatrix} \quad \text{with} \quad c_p = |W_p(t_R, f_R)| \quad (6)$$

$$\text{sign}(c_p) = \begin{cases} +1 & \text{if } |\arg(c_p) - \arg(c_1)| \approx 0 \\ -1 & \text{if } |\arg(c_p) - \arg(c_1)| \approx \pi \end{cases}, \quad \text{for } p \geq 2 \quad (7)$$

### 2.4 Step 4: Clustering of identified ridge points

In the clustering step, the identified ridge points are sorted into meaningful sets. This is done automatically with the help of clustering algorithms. Therefore, manual processing of the APS is unnecessary. Previous publication on BSS and modal identification applied well known clustering algorithms such as hierarchical clustering [15] and the centroid-based k-means clustering algorithm [14, 17, 18, 19] for the estimation of the mixing matrix. This study uses the DBSCAN algorithm by Ester et al. [20], which is an efficient density based clustering algorithm. Compared to k-means clustering this algorithm has an advantage in that the number of clusters does not have to be specified beforehand. In contrast to hierarchical clustering, this algorithm excludes outliers from the results.

Within the scope of our research on pedestrian induced vibrations, it became evident that the DBSCAN clustering is very effective and requires low computational time for a large amount of data. The control parameters for DBSCAN are a similarity radius  $\epsilon$  and a minimum number of points  $\text{minPts}$  to form a dense region. The number of points that are within a  $\epsilon$ -distance to point  $p_i$  is denoted as  $k_i$ . If  $k_i > \text{minPts}$  the point is a core point. Two points are directly connected if their distance is less than  $\epsilon$ . Two points are density connected if they are directly connected to core points and there is a chain of directly connected core points between them. Moreover, a point  $p_i$  that is directly connected to a core point but  $k_i < \text{minPts}$  is defined as a border point. Points that are neither density nor directly connected to any points are outliers. A set of all density connected points is a cluster (see Figure 2).

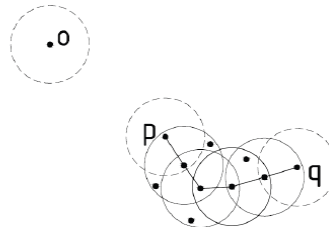


Fig. 2. DBSCAN algorithm: The points  $p$  and  $q$  are density connected border points. The point  $o$  is an outlier, which will be excluded.

The best results for analyzing the experimental data had been achieved for pedestrian induced vibrations of lightweight footbridges by applying the clustering algorithm twice. The MAC value of two mixing vectors  $\Phi_1$  and  $\Phi_2$  according to Eq. 8 can be used to compare the mixing vectors with each other, with analytical mode

shapes from finite element analysis or from separate modal identification. In the first clustering step, the MAC values are used. Here, the similarity radius  $\epsilon_{MAC}$  is set to 0.99. In the second step, the clustering algorithm is applied considering the similarity of the frequencies of the ridge points. A similarity radius of 0.1 Hz has proven suitable. After applying DBSCAN twice, the set of ridge points  $(t_R, f_R)$  is divided into  $N$  clusters such that cluster  $C_n$  consists of  $J$  points.

$$MAC(\phi_1, \phi_2) = \frac{|\phi_1^T \cdot \phi_2|^2}{\phi_1^T \cdot \phi_1 \cdot \phi_2^T \cdot \phi_2} \quad (8)$$

### 2.5 Step 5: Average frequencies, mixing vectors and Relative Energy of frequency components

Assuming that the natural frequencies, the excitation frequencies and the mixing vectors do not change significantly over time, the average frequency  $f_e(C_n)$  and the average mixing vector  $a_e(C_n)$  are calculated for each identified cluster  $C_n$ . If a cluster indicates a structural mode, the frequency  $f_e$  is the estimated natural frequency and the mixing vector  $a_e$  is an estimate for the mode shape. To evaluate the contribution of a component to the overall energy of the vibration the Relative Energy (RE) is calculated for the cluster  $C_n$  according to Eq. 9.

$$RE(C_n) = \frac{\sum_{j=1}^J APS(t_j^n, f_j^n)}{\sum_{n=1}^N \sum_{j=1}^J APS(t_j^n, f_j^n)} \quad (9)$$

## 3. Experimental studies

### 3.1 Aluminum bridge in the lab at University of Waterloo

The aluminum bridge in the laboratory located at the University of Waterloo, Canada, shown in Fig. 3 is a good test application for the proposed method. A lot of research and measurements regarding pedestrian induced vibrations have been undertaken by Dey et al. [2] using this bridge. This bridge has a span of 22.9 m and a nat. freq. of 4.59 Hz for the first vertical bending mode. The measurements for this example include one person crossing the bridge with 100 BPM (1.67 Hz) using a metronome. Six acceleration sensors are used, two at  $\frac{1}{4}$  span, two at  $\frac{1}{2}$  span and two at  $\frac{3}{4}$  span, all applied on both sides of the deck to record also torsion modes. A CWT with center frequency  $f_0 = 7$  Hz and a scale factor  $da$  of  $1/128$  is used for the TFR. The results of the new methods are presented in Fig. 4 and Table 1.



Fig. 3. Single span aluminum bridge at University of Waterloo (12.2 m version)



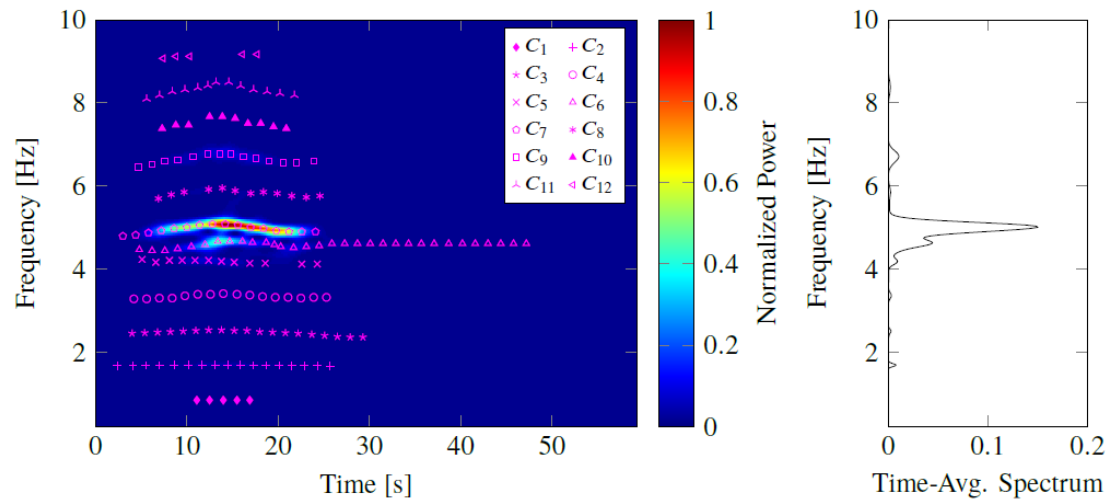


Fig. 4. APS of vibration test on the aluminum bridge with a walking person (1.67 Hz / 100 BPM) and identified cluster  $C_n$ . Note: For better readability the number of illustrated peaks is decreased by 400.

Cluster $C_n$	$f_a$ (Hz)	$f_e(C_n)$ (Hz)	RE( $C_n$ ) (%)	Description
1	-	0.84	0.2	1 <sup>st</sup> subh. exc.
2	-	1.67	2.7	excitation (step freq.)
3	-	2.46	1.1	2 <sup>nd</sup> subh. exc.
4	-	3.33	1.5	2 <sup>nd</sup> harm. exc.
5	-	4.17	4.5	3 <sup>rd</sup> subh. exc.
<b>6</b>	<b>4.59</b>	<b>4.56</b>	<b>9.8</b>	<b>1<sup>st</sup> vertical</b>
7	-	4.95	71.6	3 <sup>rd</sup> harm. exc.
8	-	5.83	1.1	4 <sup>th</sup> subh. exc.
9	-	6.62	5.4	4 <sup>th</sup> harm. exc.
10	-	7.51	0.3	5 <sup>th</sup> subh. exc.
11	-	8.30	1.4	5 <sup>th</sup> harm. exc.
12	-	9.13	0.3	6 <sup>th</sup> subh. exc.

Table 1. Identified clusters in APS of vibration test on the aluminum bridge with a walking person (1.67 Hz / 100 BPM)

The following observations were made:

- The 1<sup>st</sup> vertical bending mode at 4.56 Hz was clearly identified. The RE value of 9.8 % is comparably low. Only this frequency shows a long decay of free vibration after the person has crossed the bridge.
- The 1<sup>st</sup>, 2<sup>nd</sup>, 3<sup>rd</sup>, 4<sup>th</sup> and 5<sup>th</sup> harmonic of the excitation ( $f_e = 1.67$  Hz) can be clearly identified. All mixing vectors coincide with the first vertical bending mode.
- The 3<sup>rd</sup> harmonic of excitation (4.95 Hz) differs slightly from the theoretical value of  $3 \cdot 1.67$  Hz = 5.01 Hz and contains the highest RE value of 71.6 %. No significant change of the step frequency by the pedestrian was observed although the nat. freq. of 4.59 Hz is very close.
- The RE value of 5.4 % for the 4<sup>th</sup> harmonic of the excitation is twice as much as for 1<sup>st</sup> harmonic of the excitation. To simulate the same ratio of the RE values with a single degree of freedom (SDOF) and forced harmonic excitations the load amplitude for the 4<sup>th</sup> harmonic must be 2.5 times higher than the load amplitude for the 1<sup>st</sup> harmonic.

- The 1<sup>st</sup>, 2<sup>nd</sup>, 3<sup>rd</sup>, 4<sup>th</sup> and 5<sup>th</sup> subharmonics of the excitation can be clearly identified. All their mixing vectors show a torsion shape and not a vertical bending shape. The appearance of subharmonics of the excitation agrees well with the findings of Sahnaci [21].

### 3.2 CFRP-stress ribbon bridge at TU Berlin

The CFRP-stress ribbon bridge at the lab of TU Berlin in Fig. 5 is highly flexible and has closely spaced frequencies. This bridge has a span of 13.05 m. There are 8 concrete plates attached to six CFRP stress ribbons. Each stress ribbon has a cross section of 50 mm by 1 mm [22]. Each is pre-tensioned by a normal force of 53 kN. Sadhu et al. [23] gives further details and results of modal identification. The natural frequencies differ slightly from results here due to structural changes of the system (with and without handrail). Six acceleration sensors are used, two at  $\frac{1}{4}$  span, two at  $\frac{1}{2}$  span and two at  $\frac{3}{4}$  span applied on both sides of the deck. The vibration test has been conducted with one person crossing the bridge with 105 BPM (1.75 Hz). A CWT with a center frequency  $f_0 = 7$  Hz and a scale factor  $da = 1/128$  is used for the TFR. The results of the novel method are presented in Fig. 6 and Table 2. There is a problem with the sensor layout. The 4<sup>th</sup> vertical bending mode can hardly be found due to zero values for the mode vector at the sensor location. Different structural modes such as the 2<sup>nd</sup> mode and the 6<sup>th</sup> mode will coincide with this sensor layout, because they have the same values for the modal vector at the six sensor locations.



Fig. 5. CFRP stress ribbon bridge at TU Berlin (Schlaich [22])

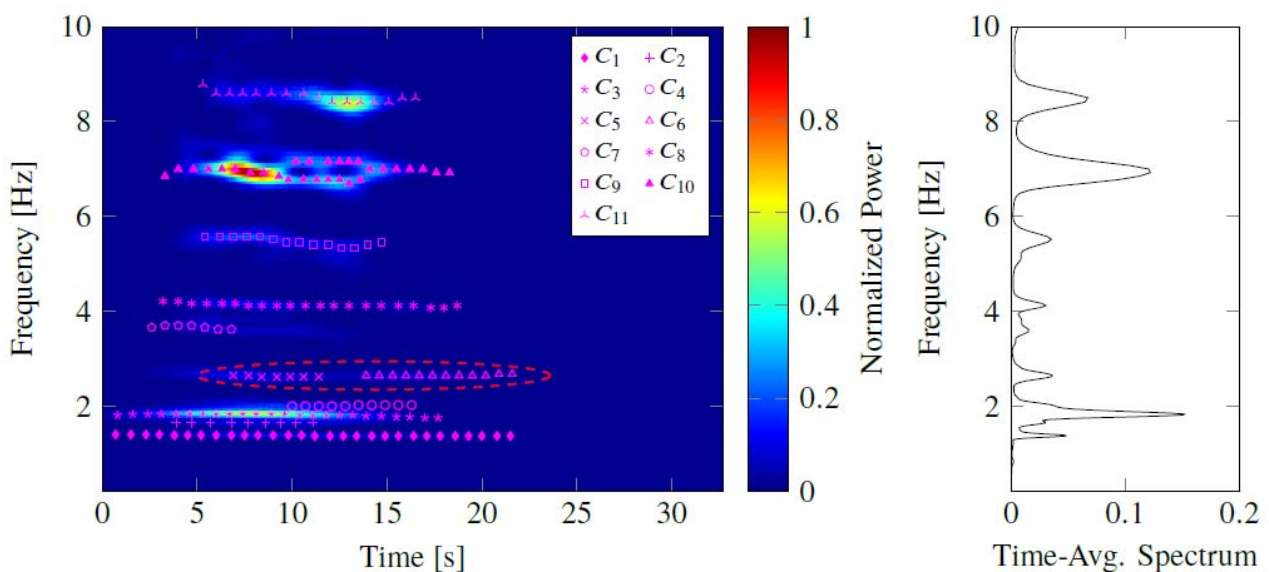


Fig. 6. APS of vibration test on the stress ribbon bridge with a walking person (1.75 Hz / 105 BPM) and identified clusters  $C_n$ . Dashed red line indicates ridge with changing mixing vector at constant frequency.



$ter\ C_n$	$f_a$ (Hz)	$f_{i1}$ (Hz)	$f_{i2}$ (Hz)	$f_e(C_n)$ (Hz)	$RE(C_n)$ (%)	$MAC(a_e(C_n), \phi_a)$ (-)	Description
1	1.44	1.38	1.40	1.37	5.1	0.99	1 <sup>st</sup> vertical mode
2	-	-	-	1.64	6.0	-	unknown
3	-	-	-	1.81	20.2	-	excitation (step freq.)
4	1.71	-	2.20	2.00	5.2	0.97	1 <sup>st</sup> torsion
5	-	-	-	2.62	6.0	-	2 subh. exc. torsion
6	2.62	-	2.69	2.64	3.6	0.98	2 <sup>nd</sup> vertical mode
7	-	-	-	3.66	3.4	-	2 <sup>nd</sup> harm. exc.
8	3.95	4.12	4.13	4.12	4.5	0.99	3 <sup>rd</sup> vertical mode
9	5.24	-	-	5.47	8.9	0.91	4 <sup>th</sup> vertical mode
10	6.55	6.95	7.00	6.95	22.0	1.00	5 <sup>th</sup> vertical mode
11	7.82	8.44	8.49	8.52	15.0	0.92	6 <sup>th</sup> vertical mode

Table 2. Identified clusters in APS and their frequencies  $f_e(C_n)$  of vibration test on the stress ribbon bridge with a walking person (1.75 Hz / 105 BPM) compared to nat. freq. by finite element model  $f_a$  and test with impact hammer ( $f_{i1}$ ,  $f_{i2}$ )

The observations of this investigation are in brief:

- The 1<sup>st</sup> and 2<sup>nd</sup> harmonic of the excitation ( $f_e = 1.81$  Hz and 3.66 Hz) are clearly identified and differ slightly from the target step frequency 1.75 Hz (105 BPM). The mixing vector of the 1<sup>st</sup> harmonic is similar to the first vertical bending mode and the mixing vector of the 2<sup>nd</sup> harmonic equals with the second vertical bending mode. Only one subharmonic of the excitation at 2.62 Hz is observed with a mixing vector of a torsional shape.
- The 1<sup>st</sup>, 2<sup>nd</sup>, 3<sup>rd</sup>, 4<sup>th</sup>, 5<sup>th</sup> and 6<sup>th</sup> natural frequencies have clear ridges in the time frequency diagram. The 5<sup>th</sup> and 6<sup>th</sup> natural frequencies are represented by clusters with high RE values of 22.0 % and 15 %. The 1<sup>st</sup> harmonic of the excitation is within the same range with an RE value of 20.2 %.
- There is one cluster at 1.64 Hz, which represents neither a natural mode nor a harmonic or subharmonic of the excitation. The frequency of 1.64 Hz is 91% of the excitation frequency  $f_{ex}$ , which lasts for a significant period. This frequency was not found in modal identification with hammer excitation or with other methods. The mixing vector looks like a linear combination of bending and torsion modes. The matter is still under investigation.
- The advantage of the two-step clustering approach becomes clear for the clusters  $C_5$  and  $C_6$ . At the beginning of the measurement, the cluster  $C_5$  at 2.62 Hz has a mixing vector with a torsional shape which corresponds to the second subharmonic at  $1.5 f_e = 2.72$  Hz. In the subsequent stages of measurement, the mixing vector changes to the second vertical bending mode with a natural frequency of 2.64 Hz. This frequency corresponds well with the results of the FE analysis. A frequency only clustering would not have identified these two clusters. In addition, the TFDD according to Le and Poulter [7] would not detect the change of the mixing vector. Moreover, the clusters  $C_1$  and  $C_3$  would not be separated if only mixing vector clustering would have been applied because their mixing vectors are similar in this sensor layout.
- The proposed method is also well suited for the identification of closely spaced frequencies. The cluster  $C_3$  at 1.81 Hz represents the 1<sup>st</sup> harmonic of the excitation and the mixing vector corresponds to the 1<sup>st</sup> vertical bending mode. The cluster  $C_4$  at 2.0 Hz represents the free vibration of the 1<sup>st</sup> torsion mode. This value agrees well with the results of the experimental modal identification by free vibration. This mode appears in the second half of the measurement period.

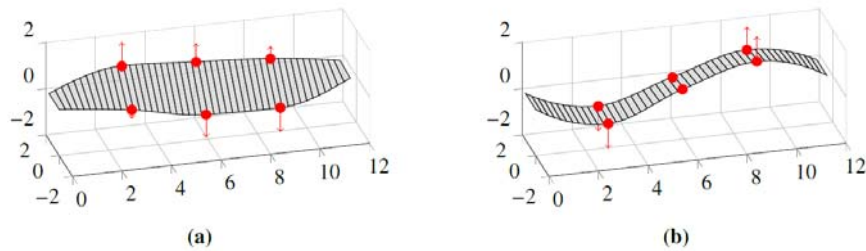


Fig. 7. Mixing vector estimates from identified clusters: (a) cluster  $C_5$ ,  $f_e = 2.62$  Hz, (b) cluster  $C_6$ ,  $f_e = 2.64$  Hz

#### 4. Discussion and Conclusions

A novel method based on time frequency analysis and clustering algorithms for analyzing vibration measurement data was presented. These clustering algorithms are applied in two steps. The first clustering step differentiates vibration components with different mixing vectors but with the same frequency. The second clustering step considering frequency similarity enables the distinction of structural modes with mode shapes that coincide due to a certain sensor layout. The novel two-step clustering approach shows significant promise in identifying different mixing vectors due to forced and free vibration occurring at frequencies close to each other.

Pedestrian walking is a complex excitation especially for lightweight bridges. It is multi – narrow banded, not stationary and there are often closely spaced natural frequencies especially with cable-supported bridges. This method is shown to be an excellent tool for analyzing the measurement data to understand characteristic of the excitation, for comparing the quality of load models with real excitation in the time-frequency domain and for identifying modal properties of structures such as natural frequencies and mode shapes. In contrast to frequency or time-only domain methods, it is also possible to detect and visualize transient oscillatory components as well as the change of frequencies and mode shapes over time.

The proposed method was applied to two examples of pedestrian induced vibrations: an aluminum truss bridge and a CFRP-stress ribbon bridge. Natural frequencies as well as harmonics and sub-harmonics of the excitation frequency have been identified. The accompanying shape of the mixing vectors coincide very well with the mode shapes of these footbridges. Even for the forced vibration the shape of the mixing vector were identified. An important result was that higher structural modes and higher harmonics of the step frequency can concentrate a significant amount of vibrational energy, which is often ignored in many codes and guidelines.

#### 4.1 References

- [1] HEINEMEYER C., et al.: Hivoss – Human induced vibrations of steel structures. [http:// www.stb.rwth-aachen.de/projekte/2007/HIVOSS/download.php](http://www.stb.rwth-aachen.de/projekte/2007/HIVOSS/download.php) and
- [2] DEY P., NARASIMHAN S., WALBRIDGE S., "Evaluation of Design Guidelines for the Serviceability Assessment of Aluminum Pedestrian Bridges." *Journal of Bridge Engineering* 22.1 (2016): 04016109.
- [3] SADHU, A., NARASIMHAN, S., ANTONI, J. "A review of output-only structural mode identification literature employing blind source separation methods." *Mechanical Systems And Signal Processing* 94 (2017): 415-431.
- [4] LARDIES J. and GOUTTEBROZE S., "Identification of modal parameters using the wavelet transform." *International Journal for Mechanical Sciences*, 44 (2002), 2263 – 2283.
- [5] KIJEWSKI T. and KAREEM A., "Wavelet transform for system identification in civil engineering," *Computer-Aided Civil and Infrastructure Engineering*, Vol.18, (2003), pp. 339 –355.
- [6] NAGARAJIAH S. and BASU B., "Output only modal identification and structural damage detection using time frequency & wavelet techniques." *Earthquake engineering and engineering vibration*, 8(4), 2009, 583 – 605.

- [7] LE, T.-P., PAULTRE, P., "Modal identification based on the time-frequency domain decomposition of unknown-input dynamic tests." *International Journal for Mechanical Sciences*, Vol. 71, 2013, pp. 41 - 50.
- [8] GHAHARI S. F., ABAZARSA F., GHANNAD M. A., CELEBI M., and TACIROGLU E., "Blind modal identification of structures from spatially sparse seismic response signals," *Structural Control and Health Monitoring*, Vol.21, 2014, pp.649–674.
- [9] ALLEN J., "Short Term Spectral Analysis, Synthesis, and Modification by Discrete Fourier Transform," *Transactions on Acoustics, Speech and Signal Processing*, 1977.
- [10] TORRENCE C. and COMPO G. P., "A practical guide to wavelet analysis," *Bulletin of the American Meteorological society*, Vol.79, No.1, 1998, pp.61–78.
- [11] STOCKWELL R., MANSINHA L. and LOWE R., "Localization of the Complex Spectrum: The S-Transform," *IEEE Transactions on Signal Processing*, 1996.
- [12] CHANDRE, C., WIGGINS, S., and UZER, T., "Time-frequency analysis of chaotic systems." 482 *Physica D*, 181, 2003, pp. 171 – 196.
- [13] LE T.-P. and ARGOU L., "Continuous wavelet transform for modal identification using free decay response," *Journal for Sound and Vibration*, Vol. 277, 2004, pp.73–100.
- [14] RAINIERI C. and FABBROCINO G., "Operational modal analysis of civil engineering structures," tech. rep., Springer, 2014.
- [15] REJU V., KOH S. N., and SOON I., "An algorithm for mixing matrix estimation in instantaneous blind source separation," *Signal Processing*, Vol. 89, 2009, pp.1762–1773.
- [16] TODOROVSKA, M., Estimation of instantaneous frequency of signals using the continuous wavelet transform. University of Southern California, Department of Civil Engineering, 2001.
- [17] SMITH D., LUKASIAK J. and BURNETT I. S., "A two channel, block-adaptive audio separation technique based upon time-frequency information," *Signal Processing Conference*, Vol.12<sup>th</sup> European, 2004, pp.393–396.
- [18] KIM S. and YOO C.D., "Underdetermined blind source separation based on subspace representation," *IEEE Transactions on Signal Processing*, Vol.57, No. 7, 2009, pp.2604– 2614.
- [19] YANG Y. and NAGARAJIAH S., "Time-frequency blind source separation using independent component analysis for output-only modal identification of highly damped structures," *Journal of Structural Engineering*, Vol. 139, No. 10, 2013, pp. 1780 – 1793.
- [20] ESTER M., KRIEGER H.-P., SANDER J. and XU X. "A Density-Based Algorithm for Discovering Clusters in Large Spatial Data bases with Noise." *Proceedings of 2<sup>nd</sup> International Conference on Knowledge Discovery and Data Mining*, 1996.
- [21] SAHNACI, C., Menscheninduzierte Einwirkungen auf Tragwerke infolge der Lokomotionsformen Gehen und Rennen : Analyse und Modellierung. Ph.D thesis, 2013 (in German).
- [22] SCHLAICH M., BLEICHER A., Spannbandbrücke mit Kohlenstofffaser-Lamellen. *Bautechnik* 84, Heft 5, pp. 311–319, 2007 (in German).
- [23] SADHU A., GOLDACK A. AND NARASIMHAN S., "Blind Modal Identification of a Pedestrian Bridge under Narrowband Disturbances". *Proceedings of the 9<sup>th</sup> International Conference on Structural Dynamics*, EUROLYN, 2014.